Signal Processing 172 (2020) 107428

Contents lists available at ScienceDirect

Signal Processing

journal homepage: www.elsevier.com/locate/sigpro

Improved two-dimensional DOA estimation using parallel coprime arrays

Si Qin[a], Yimin D. Zhang[b,*], Moeness G. Amin[c]

[a] Microsoft Research Asia, Beijing 100080, China
[b] Department of Electrical and Computer Engineering, Temple University, Philadelphia, PA 19122, USA
[c] Center for Advanced Communications, Villanova University, Villanova, PA 19085, USA

ARTICLE INFO

Article history:
Received 10 April 2019
Revised 23 October 2019
Accepted 9 December 2019
Available online 10 December 2019

Keywords:
Two-dimensional direction-of-arrival estimation
Coprime array
Sparse array
Parallel subarray
Compressive sensing

ABSTRACT

The conventional coprime array consists of two uniform linear subarrays to construct an effective difference coarray with desirable characteristics. Such linear coprime arrays only provide one-dimensional (1-D) direction-of-arrival (DOA) estimation. In this paper, we propose a novel coprime array configuration with parallel subarrays, along with an effective method for two-dimensional (2-D) DOA estimation. The 2-D DOA estimation problem is cast as two separate 1-D problems for reduced complexity and is solved using one of the two mechanisms based on the number of sensors and that of sources. When there are less sources than the number of sensors, subspace-based and rank-reduction estimation (RARE) techniques are sequentially applied to the physical array output. On the other hand, when the number of sources is equal to or larger than that of sensors, a virtual difference coarray is formed and group sparse reconstruction and least squares operations are then applied. In both scenarios, the proposed methods automatically pair the corresponding azimuth and elevation angles. The proposed methods resolve up to MN sources using $2M+N-1$ sensors, which are the same as in the 1-D DOA estimation using conventional coprime arrays. Simulations results are presented delineating both the accuracy and resolution capability of the proposed method.

1. Introduction

Direction-of-arrival (DOA) estimation determines the spatial spectrum of the impinging electromagnetic waves on a sensor array. It finds variety of applications in radar, sonar, radio astronomy, and mobile communication systems [1]. A large volume of work has investigated linear arrays for one-dimensional (1-D) DOA estimation, namely, the azimuth domain. Among existing DOA estimation techniques, the multiple signal classification (MUSIC) [2], estimation of signal parameters via rotational invariance techniques (ESPRIT) [3], and propagator method (PM) [4] are commonly used due to their high-resolution direction finding capabilities utilizing eigen-value decomposition (EVD), singular value decomposition (SVD), and linear operations with respect to the estimated covariance matrix of the received signals, respectively. Recently, super-resolution algorithms are proposed for massive MIMO based on deep learning [5]. In practice, however, many problems require two-dimensional (2-D) DOA estimation in both azimuth and elevation domains. While it is straightforward to extend the above methods to their 2-D counterparts [6–8] to deal with a planar or circular array, the involved 2-D peak search is computationally expensive, especially for large number of sensors. Therefore, it is desirable to develop an accurate 2-D DOA estimation algorithm with reduced complexity.

Several methods for 2-D DOA estimation problem were proposed with parallel uniform linear array (ULA) configurations that consist of several linear subarrays, converting the problem into separate 1-D DOA estimations. In doing so, either the PM based [9–12] or subspace based [13] algorithm can be applied to estimate only one variable, avoiding 2-D angular search. In [9], a fast algorithm was proposed based on two parallel ULAs with N and $N+1$ sensors. The resulting configuration lends itself to formulating three N-sensor subarrays where the azimuth and elevation angles can be estimated separately. However, an additional pair matching process for the estimated azimuth and elevation angles is required when multiple sources exist. In addition, the total number of sensors, i.e., $N_t = 2N+1$, is not fully utilized in each estimation stage. The method developed in [10] considers the same two parallel ULA structure as used in [9], but it automatically pairs the 2-D DOA estimates and achieves improved DOA estimation accuracy by constructing three $2N$-sensor subarrays rather than the

* Corresponding author.
E-mail addresses: yimin@ieee.org, ydzhang@temple.edu (Y.D. Zhang).

https://doi.org/10.1016/j.sigpro.2019.107428
0165-1684/

N-sensor counterparts in [9]. Nevertheless, it still falls short in utilizing all degrees-of-freedoms (DOFs) offered by the array sensors. In addition, the array configuration used in [9,10] assumes a small aperture in the elevation domain owing to the half-wavelength distance constraint between the parallel ULAs which circumvents creation of grating lobes. Therefore, the performance of the above methods degrades significantly with high elevation angles, which is typical in mobile communication environments. The methods in [11,12] enlarge the aperture in the elevation domain by exploiting three parallel ULAs. However, the number of DOFs in these methods remains lower than half of the number of sensors (i.e., $N_t/2$), limiting the possible number of resolvable sources. A method was proposed in [13] based on the MUSIC technique. Particularly, the rank-reduction (RARE) estimator [14] was applied enabling the three parallel ULAs to be treated as subarrays displaced from a long ULA, and allowing the resolution of up to $(N_t - 3)$ sources. Clearly, such a ULA-based parallel array design imposes a strict restriction on the array aperture and does not achieve a high number of DOFs.

For detecting more sources than sensors, it is necessary to have a higher number of DOFs which can be achieved by exploiting a sparse array configuration under the coarray equivalence [15,16]. A sparse array also renders a larger array aperture for high resolution spatial spectrum estimation. Among the different techniques for sparse array construction, the recently proposed coprime configurations [17,18] and nested configuration [19] offer systematical design capability and DOF analysis involving sensors, samples, or frequencies [20–43].

The conventional coprime array developed in [18] consists of two collocated uniform linear subarrays, where one uses $2M$ antennas with an interelement spacing of N units, whereas the other one uses N elements with an interelement spacing of M units. By choosing the integer numbers M and N to be coprime, i.e., their greatest common divisor is one, MN sources can be identified with only $2M + N - 1$ sensors. A variety of coprime array configurations were developed to achieve higher DOFs and more flexible array design [44]. However, the above coprime arrays are limited to the 1-D case. In [45], we proposed a coprime array configuration for the 2-D DOA estimation, where the two subarrays are placed in parallel rather than co-linearly. The resulting configuration is able to resolve the same number of sources in the 2-D DOA domain as compared with the conventional linear coprime array with the same number of sensors for 1-D DOA estimation. A similar problem was investigated in [46,47]. However, all these methods have difficulties to resolve the sources with high elevation angles.

In this paper, we propose a novel coprime array configuration with three parallel subarrays for 2-D DOA estimation. Unlike the methods in [11] and [12] where each of the three parallel subarrays is uniform, the proposed method undertakes a sparse array topology to resolve a significantly higher number of sources. In addition, the proposed array configuration outperforms the methods in [45–47] given the same number of DOFs. From array design perspective, the extended array aperture in the proposed array configuration improves resolution in the elevation domain. Such offering is more pronounced for high elevation angles. From an algorithmic perspective, we propose an effective method to perform 2-D DOA estimation. The problem is similarly cast as two separate 1-D DOA estimations, with adopting two different schemes depending on the number of sensors, N_t, and sources, Q. More specifically, for the case of $Q < N_t$, the MUSIC and RARE techniques are sequentially applied to the data received at the physical array, whereas when $Q \geq N_t$, a virtual difference coarray is first formed from the cross-covariance matrix of the subarray data, and group sparse reconstruction and least squares operations are then used to estimate the 2-D DOAs. In both schemes, the proposed method achieves improved DOA estimation accuracy and properly pairs the source azimuth and elevation angles.

The rest of the paper is organized as follows. In Section 2, we describe the signal model of the proposed coprime array configuration with parallel subarrays. In Section 3, an effective DOA estimation method is presented in two different cases based on the relationship between N_t and Q. Simulation results are provided in Section 4 to numerically compare the estimation performance of the proposed method with those of existing methods. Section 5 concludes the paper.

Notions: We use lower-case (upper-case) bold characters to denote vectors (matrices). In particular, $\mathbf{I}_N$ denotes the $N \times N$ identity matrix, and $\mathbf{1}_{1\times N}$ and $\mathbf{0}_{1\times N}$ denote $1 \times N$ vectors with all 1's and 0's, respectively. $(.)^*$ implies complex conjugation, whereas $(.)^T$ and $(.)^H$ respectively denote the transpose and conjugate transpose of a matrix or vector. vec$(\cdot)$ denotes the vectorization operator that turns a matrix into a vector by stacking all columns on top of the another, and diag($\mathbf{x}$) denotes a diagonal matrix that uses the elements of $\mathbf{x}$ as its diagonal elements. E$(\cdot)$ is the statistical expectation operator and $\otimes$ denotes the Kronecker product. phase(x) returns the phase of a complex variable x. $\mathbb{N}^+$ denotes the set of positive integers. $\lfloor \cdot \rfloor$ denotes the floor function that returns the largest integer not exceeding the argument. $\mathcal{N}(x|a, b)$ and $\mathcal{CN}(x|a, b)$ denote that random variable x follows Gaussian and complex Gaussian distributions with mean a and variance b, respectively. $\|\cdot\|_2$ denotes the Euclidean (l_2). Tr($\mathbf{A}$) and and $|\mathbf{A}|$ respectively returns the trace and determinant of matrix $\mathbf{A}$. Re(x) and Im(x) denote the real and imaginary parts of complex element x, respectively.

2. Array configuration and signal model

As illustrated in Fig. 1, the proposed coprime array configuration consists of three sparse ULAs. The subarray 1 has N sensors with an interelement spacing of Md, whereas the subarray 2 and 3 have $M - 1$ and M sensors, respectively, with an interelement spacing of Nd. The unit interelement spacing d is set to $\lambda/2$, where the λ is the wavelength corresponding to the carrier frequency. By choosing the $M \in \mathbb{N}^+$ and $N \in \mathbb{N}^+$ to be coprime, the minimum interelement spacing along the y-axis remains $\lambda/2$ so as to avoid grating lobes in the azimuth domain. Without loss of generality, we assume $M < N$ in this paper. The array sensors are positioned at:

$$\{(x, y)|(0, Mnd) \cup (d, Nm_1 d) \cup (d + Ld, MNd + Nm_2 d)\} \tag{1}$$

for all $n \in [0, N-1]$, $m_1 \in [1, M-1]$, $m_2 \in [0, M-1]$, $n, m_1, m_2 \in \mathbb{N}^+$, where (x, y) denotes the coordinate in $x - y$ plane. Note that the difference to the conventional coprime arrays for the 1-D DOA estimation lies in the fact that these subarrays are no longer co-linear, but are rather placed in parallel with a distance d and $Ld, L \in \mathbb{N}^+$, respectively. On one hand, the minimum interelement spacing along the x-axis, i.e., d, guarantees free of the ambiguous problem in the elevation domain. Furthermore, the width of its mainlobe is inversely proportional to the x-axis array aperture L_x. As L increases, the resolution improves as a result of the narrower mainlobe. However, the corresponding spatial spectrum, which generally describes spatial correlation with respect to the elevation grids, tends to include high-level sidelobes as the array aperture increases. Therefore, it is undesirable to use an extremely large value of L because it will lead to a deteriorated estimation accuracy due to the effect of spurious peaks caused by the corresponding high sidelobe levels.

Assume that Q far-field narrowband uncorrelated sources $s_q(t)$, $q = 1, \ldots, Q$, for $t = 1, \ldots, T$, impinge on the array from the pair of 2-D angles (θ_q, ϕ_q), where $\theta_q \in [0^\circ, 90^\circ]$ and $\phi_q \in [-180^\circ, 180^\circ]$ denote the elevation angle and the azimuth angle corresponding to

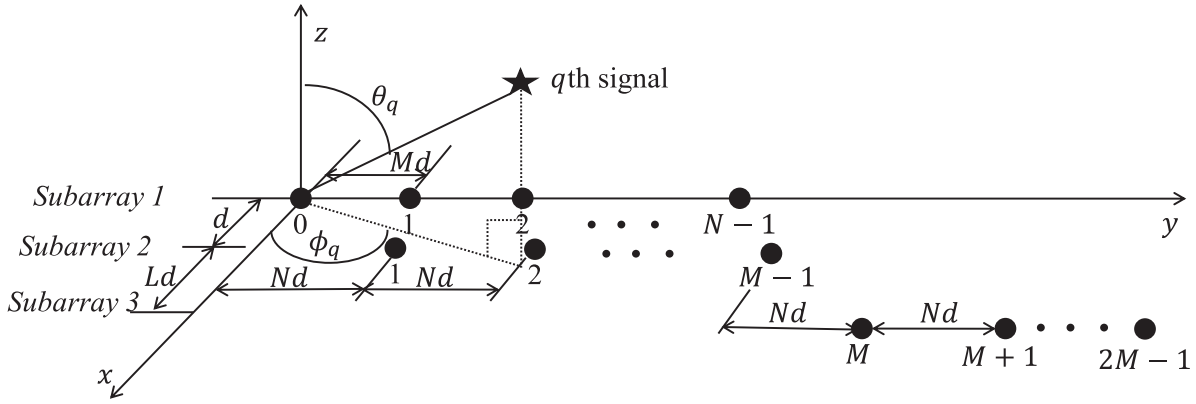

Fig. 1. Geometry of the proposed array configuration with three parallel coprime subarrays.

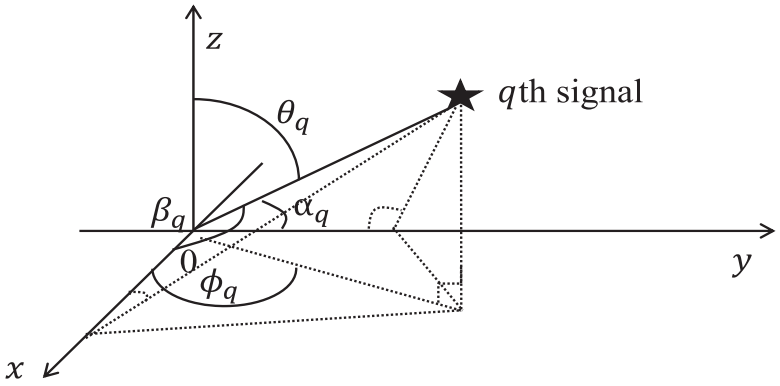

Fig. 2. Illustration on relationships between (θ_q, ϕ_q) and (α_q, β_q).

the qth signal, respectively. Then, the data vectors received at the ith subarray can be expressed as

$$\mathbf{x}_i(t) = \sum_{q=1}^{Q} \mathbf{a}_i(\theta_q, \phi_q) e^{j2\pi \frac{x_i}{\lambda} \sin(\theta_q)\cos(\phi_q)} s_q(t) + \mathbf{n}_i(t), \tag{2}$$

where

$$\mathbf{a}_i(\theta_q, \phi_q) = \left[e^{j2\pi \frac{y_1^i}{\lambda} \sin(\theta_q)\sin(\phi_q)}, \ldots, e^{j2\pi \frac{y_{N_t^i}^i}{\lambda} \sin(\theta_q)\sin(\phi_q)} \right]^T, \tag{3}$$

is the steering vector of the ith subarray corresponding to the pair of (θ_q, ϕ_q) for $q = 1, \ldots, Q$, $i = 1, 2, 3$. y_j^i, $1 \le j \le N_t^i$, denotes the y-coordinate of the jth sensor in the ith subarray, where N_t^i is the total number of sensors in the ith subarray, i.e., $N_t^1 = N$, $N_t^2 = M - 1$, and $N_t^3 = M$. Similarly, x_i represents the position of the ith subarray along the x-axis. In addition, the elements of the noise vectors in the ith subarray $\mathbf{n}_i(t)$ are assumed to be independent and identically distributed (i.i.d.) random variables following the complex Gaussian distribution $\mathcal{CN}(0, \sigma_n^2 \mathbf{I}_{N_t^i})$ for $i = 1, 2, 3$.

In order to decouple the 2-D DOA estimation problem into two separated 1-D problems, as shown in Fig. 2, we define α_q, $\beta_q \in [0^\circ, 180^\circ]$, $q = 1, \ldots, Q$, as the angles between the incident direction and the y-axis and the x-axis, respectively. α_q and β_q are related with θ_q and ϕ_q through the following relationships:

$$\cos(\alpha_q) = \sin(\theta_q)\sin(\phi_q), \tag{4}$$

$$\cos(\beta_q) = \sin(\theta_q)\cos(\phi_q). \tag{5}$$

As a result, the received data vectors in (2) becomes

$$\mathbf{x}_i(t) = \sum_{q=1}^{Q} \mathbf{a}_i(\alpha_q) e^{j2\pi \frac{x_i}{\lambda} \cos(\beta_q)} s_q(t) + \mathbf{n}_i(t), \tag{6}$$

with the corresponding steering vector

$$\mathbf{a}_i(\alpha_q) = \left[e^{j2\pi \frac{y_1^i}{\lambda} \cos(\alpha_q)}, \ldots, e^{j2\pi \frac{y_{N_t}^i}{\lambda} \cos(\alpha_q)} \right]^T. \tag{7}$$

Denote $\mathbf{s}(t) = [s_1(t), \ldots, s_Q(t)]^T$ as the signal vector, and $\mathbf{A}_i = [\mathbf{a}_i(\alpha_1), \ldots, \mathbf{a}_i(\alpha_Q)]$, as the corresponding manifold of the ith subarray, $i = 1, 2, 3$. Then, the received data vectors can be rewritten as

$$\mathbf{x}_i(t) = \mathbf{A}_i \mathbf{B}_i \mathbf{s}(t) + \mathbf{n}_i(t), \tag{8}$$

where the diagonal matrix is expressed as

$$\mathbf{B}_i = \mathrm{diag}\left(\left[e^{j2\pi \frac{x_i}{\lambda} \cos(\beta_1)}, \ldots, e^{j2\pi \frac{x_i}{\lambda} \cos(\beta_Q)} \right] \right). \tag{9}$$

3. Proposed DOA estimation method: $Q < N_t$ case

In this and the subsequent sections, we present an effective approach for the 2-D DOA estimation using the proposed array configuration. In the light of the relationship between Q and N_t, two different cases are considered with distinct mechanisms. In this section, we address the case where $Q < N_t$, whereas the case of $Q \ge N_t$ is considered in Section 4. In both cases, the proposed method automatically pairs the 2-D angles and achieves improved estimation accuracy over existing techniques.

When $Q < N_t$, the DOA estimation is based on the N_t-sensor physical array. Stacking all data vectors received at

the three subarrays $\mathbf{x}_i(t), i = 1, 2, 3$, yields an $N_t \times 1$ vector $\mathbf{x}(t) = [\mathbf{x}_1^T(t), \mathbf{x}_2^T(t), \mathbf{x}_3^T(t)]^T$, where $\mathbf{x}_1(t) \in \mathbb{C}^{N\times 1}$, $\mathbf{x}_2(t) \in \mathbb{C}^{(M-1)\times 1}$, $\mathbf{x}_3(t) \in \mathbb{C}^{M\times 1}$, and $N_t = 2M + N - 1$. As such, the $\mathbf{x}(t)$ is treated as the received data vector of a long linear array, expressed as:

$$\mathbf{x}(t) = \sum_{q=1}^{Q} \mathbf{a}(\alpha_q, \beta_q) s_q(t) + \mathbf{n}(t) = \mathbf{C}\mathbf{s}(t) + \mathbf{n}(t), \tag{10}$$

with

$$\mathbf{a}(\alpha_q, \beta_q) = \tilde{\mathbf{a}}(\alpha_q)\mathbf{T}\mathbf{h}(\beta_q), \tag{11}$$

where

$$\tilde{\mathbf{a}}(\alpha_q) = \mathrm{diag}\big([\mathbf{a}_1^T(\alpha_q)\ \mathbf{a}_2^T(\alpha_q)\ \mathbf{a}_3^T(\alpha_q)]^T\big), \tag{12}$$

$$\mathbf{T} = \begin{bmatrix} \mathbf{1}_{1\times N}\mathbf{0}_{1\times(M-1)}\mathbf{0}_{1\times M} \\ \mathbf{0}_{1\times N}\mathbf{1}_{1\times(M-1)}\mathbf{0}_{1\times M} \\ \mathbf{0}_{1\times N}\mathbf{0}_{1\times(M-1)}\mathbf{1}_{1\times M} \end{bmatrix}^T, \tag{13}$$

$$\mathbf{h}(\beta_q) = \left[1, e^{j\pi\cos(\beta_q)}, e^{j(L+1)\pi\cos(\beta_q)}\right]^T. \tag{14}$$

Note that the azimuth and elevation angles α_q and β_q in the corresponding $N_t \times 1$ steering vector $\mathbf{a}(\alpha_q, \beta_q)$ can be decoupled as the product of an $N_t \times N_t$ diagonal matrix $\tilde{\mathbf{a}}(\alpha_q)$, which only depends on α_q, a 3×1 steering vector $\mathbf{h}(\beta_q)$, which only depends on β_q, and an $N_t \times 3$ transformation matrix $\mathbf{T}$. As such, an exhaustive 2-D search is avoided. The $N_t \times Q$ matrix $\mathbf{C}$ is defined as the mainfold corresponding to all steering vectors $\mathbf{a}(\alpha_q, \beta_q)$ for $q = 1, \ldots, Q$, expressed as

$$\mathbf{C} = [\mathbf{a}(\alpha_1, \beta_1), \ldots, \mathbf{a}(\alpha_Q, \beta_Q)] = \left[(\mathbf{A}_1\mathbf{B}_1)^T, (\mathbf{A}_2\mathbf{B}_2)^T, (\mathbf{A}_3\mathbf{B}_3)^T\right]^T. \tag{15}$$

In addition, the corresponding $N_t \times 1$ noise vector is denoted as $\mathbf{n}(t) = [\mathbf{n}_1^T(t), \mathbf{n}_2^T(t), \mathbf{n}_3^T(t)]^T$. The $N_t \times N_t$ covariance matrix of the received data vector $\mathbf{x}(t)$ is obtained as

$$\mathbf{R}_\mathbf{x} = \mathrm{E}[\mathbf{x}(t)\mathbf{x}^H(t)] = \mathbf{C}\mathbf{R}_{\mathbf{ss}}\mathbf{C}^H + \sigma_n^2\mathbf{I}_{N_t}. \tag{16}$$

Following the same process in 2-D MUSIC [6], the signal and noise subspaces can be estimated via eigenvalue decomposition with respect to the covariance matrix, i.e.,

$$\mathbf{R}_\mathbf{x} = \mathbf{U}_s\mathbf{\Lambda}_s\mathbf{U}_s^H + \mathbf{U}_n\mathbf{\Lambda}_n\mathbf{U}_n^H, \tag{17}$$

where the $N_t \times Q$ matrix $\mathbf{U}_s$ and the $N_t \times (N_t - Q)$ matrix $\mathbf{U}_n$ contain the signal and noise subspace eigenvectors, respectively, and the corresponding eigenvalues are included in the diagonal matrices $\mathbf{\Lambda}_s = \mathrm{diag}\{\lambda_1, \ldots, \lambda_Q\}$ and $\mathbf{\Lambda}_n = \mathrm{diag}\{\lambda_{Q+1}, \ldots, \lambda_{N_t}\}$. Then, the cost function for MUSIC-based DOA estimation can be constructed as

$$\begin{aligned} f(\alpha_{g_1}, \beta_{g_2}) &= \frac{1}{\mathbf{a}^H(\alpha_{g_1}, \beta_{g_2})\mathbf{U}_n\mathbf{U}_n^H\mathbf{a}(\alpha_{g_1}, \beta_{g_2})} \\ &= \frac{1}{\mathbf{h}^H(\beta_{g_2})\mathbf{T}^H\tilde{\mathbf{a}}^H(\alpha_{g_1})\mathbf{U}_n\mathbf{U}_n^H\tilde{\mathbf{a}}(\alpha_{g_1})\mathbf{T}\mathbf{h}(\beta_{g_2})} \\ &= \frac{1}{\mathbf{h}^H(\beta_{g_2})\mathbf{G}(\alpha_{g_1})\mathbf{h}(\beta_{g_2})}, \end{aligned} \tag{18}$$

with $\mathbf{G}(\alpha_{g_1}) = \mathbf{T}^H\tilde{\mathbf{a}}^H(\alpha_{g_1})\mathbf{U}_n\mathbf{U}_n^H\tilde{\mathbf{a}}(\alpha_{g_1})\mathbf{T}$, where $g_1 = 1, \ldots, G_\alpha$, and $g_2 = 1, \ldots, G_\beta$ denotes the search grids for angles α and β. In (18), the difference to the counterpart in the traditional 2-D MUSIC method that applied to a planar or circular array lies in the fact that α_{g_1} and β_{g_2} are fully decoupled, which means that the joint 2-D searching $(\alpha_{g_1}, \beta_{g_2})$ is not necessary when maximizing $f(\alpha_{g_1}, \beta_{g_2})$ to obtain the Q largest peaks. In other words, the estimation of α_q and β_q, $q = 1, \ldots, Q$, can be simplified as two separate 1-D DOA estimation problems. We first apply the RARE algorithm to estimate α_q by maximizing the following cost function

$$f(\alpha_{g_1}) = \frac{1}{|\mathbf{G}(\alpha_{g_1})|}, \quad g_1 = 1, \ldots, G_\alpha. \tag{19}$$

As such, the estimates of α_q, i.e., $\hat{\alpha}_q$, $q = 1, \ldots, Q$, can be obtained by detecting the positions of the Q largest peaks in $f(\alpha_g)$. Given each $\hat{\alpha}_q$, we then perform a 1-D search with respect to β, i.e.,

$$f(\hat{\alpha}_q, \beta_{g_2}) = \frac{1}{\mathbf{h}^H(\beta_{g_2})\mathbf{G}(\hat{\alpha}_q)\mathbf{h}(\beta_{g_2})}, \quad g_2 = 1, \ldots, G_\beta. \tag{20}$$

The evaluation angles $\hat{\beta}_q$ are identified by the angular positions of peaks, which are automatically paired with the corresponding $\hat{\alpha}_q$, $q = 1, \ldots, Q$.

Based on the relationship between (θ_q, ϕ_q) and (α_q, β_q) in (4) and (5), the elevation and azimuth angle for each source can be estimated as

$$\hat{\theta}_q = \sin^{-1}\left[\sqrt{\cos^2(\hat{\alpha}_q) + \cos^2(\hat{\beta}_q)}\right], \tag{21}$$

$$\hat{\phi}_q = \tan^{-1}\left[\frac{\cos(\hat{\alpha}_q)}{\cos(\hat{\beta}_q)}\right]. \tag{22}$$

It is clear that θ_q and ϕ_q are also automatically paired due to the paired α_q and β_q.

4. Proposed DOA estimation method: $Q \geq N_t$ case

While the RARE and MUSIC can achieve a high resolution in the spectrum and improved estimation accuracy, the $Q < N_t$ condition has to be satisfied so as to obtain the noise subspace. The problem of detecting more sources than the number of sensors is of tremendous interests in various applications. In this section, we present an effective approach to achieve a higher number of DOFs under the difference coarray equivalence. In addition, both resolution and estimation accuracy are improved by exploiting the group sparse learning techniques.

4.1. Difference coarray formulation

The cross-covariance matrix between the data vectors received at subarrays, $\mathbf{x}_i(t)$ and $\mathbf{x}_k(t)$, $1 \leq i, k \leq 3$, can be obtained as

$$\begin{aligned} \mathbf{R}_{\mathbf{x_{ik}}} &= \mathrm{E}[\mathbf{x}_i(t)\mathbf{x}_k^H(t)] \\ &= \sum_{q=1}^{Q} \sigma_q^2 e^{j2\pi\frac{(x_i - x_k)}{\lambda}\cos(\beta_q)}\mathbf{a}_i(\alpha_q)\mathbf{a}_k^H(\alpha_q) + \mathbf{n}_i(t)\mathbf{n}_k^H(t), \\ &= \begin{cases} \mathbf{A_i}\mathbf{R_{ss}}\mathbf{D_{ik}}\mathbf{A_k^H}, & i \neq k, \\ \mathbf{A_i}\mathbf{R_{ss}}\mathbf{A}_i^H + \sigma_n^2\mathbf{I}_{N_i}, & i = k, \end{cases} \end{aligned}$$

where $\mathbf{R_{ss}} = \mathrm{E}[\mathbf{s}(t)\mathbf{s}^H(t)] = \mathrm{diag}([\sigma_1^2, \ldots, \sigma_Q^2])$ is the $Q \times Q$ covariance matrix of the signals whose diagonal entries represent the signal scattering power. In addition,

$$\mathbf{D}_{ik} = \mathbf{B}_i\mathbf{B}_k^H = \mathrm{diag}\left\{\left[e^{j2\pi\frac{(x_i - x_k)}{\lambda}\cos(\beta_1)}, \ldots, e^{j2\pi\frac{(x_i - x_k)}{\lambda}\cos(\beta_Q)}\right]^T\right\}, \tag{24}$$

which becomes the identity matrix when $i = k$.

By vectorizing the matrix $\mathbf{R}_{\mathbf{x}_{ik}}$, we obtain the following measurement vector:

$$\mathbf{z}_{ik} = \mathrm{vec}(\mathbf{R}_{\mathbf{x}_{ik}}) = \begin{cases} \bar{\mathbf{A}}_{\mathbf{ik}}\mathbf{b}_{\mathbf{ik}}, & i \neq k, \\ \bar{\mathbf{A}}_{ik}\mathbf{b}_{ik} + \sigma_n^2\mathbf{i}, & i = k, \end{cases} \tag{25}$$

with

$$\bar{\mathbf{A}}_{ik} = [\tilde{\mathbf{a}}_{ik}(\alpha_1), \ldots, \tilde{\mathbf{a}}_{ik}(\alpha_Q)], \tag{26}$$

$$\mathbf{b}_{ik} = \left[\sigma_1^2 e^{j2\pi\frac{(x_i - x_k)}{\lambda}\cos(\beta_1)}, \ldots, \sigma_Q^2 e^{j2\pi\frac{(x_i - x_k)}{\lambda}\cos(\beta_Q)}\right]^T, \tag{27}$$

where $\tilde{\mathbf{a}}_{ik}(\alpha_q) = \mathbf{a}_i(\alpha_q) \otimes \mathbf{a}_k^*(\alpha_q)$ for $1 \leq q \leq Q$, and $\mathbf{i} = \mathrm{vec}(\mathbf{I}_{N_i})$. Benefiting from the Vandermonde structure of vectors $\mathbf{a}_i(\alpha_q)$ and

$\mathbf{a}_k(\alpha_q)$, the entries in $\bar{\mathbf{a}}_{ik}(\alpha_q)$ remain the forms of $e^{j\pi(Mn-Nm)\cos(\alpha_q)}$. Therefore, $\mathbf{z}_{ik}$ can be regarded as a data vector received from a single-snapshot signal vector $\mathbf{b}_{ik}$, and the manifold $\bar{\mathbf{A}}_{ik}$ corresponds to a virtual array whose virtual elements are located at the self- and cross-lags between different sets of subarrays. Due to the co-prime property of M and N, there are less redundant elements in these virtual arrays. As a consequence, the number of DOFs in the resulting coarray, which is determined by the cardinality of the unique sum of self-lags and cross-lags, can be substantially increased, thereby enabling DOA estimation of more signals than the number of sensors, i.e., N_t.

4.2. Sparsity-based DOA estimation

The signal vector in (25), $\mathbf{z}_{ik}$, $1 \le i, k \le 3$, can be sparsely represented over the entire discretized angular grids as

$$\mathbf{z}_{ik} = \begin{cases} \bar{\mathbf{A}}^{\circ}_{\mathbf{ik}}\mathbf{b}^{\circ}_{\mathbf{ik}}, & i \neq k, \\ \bar{\mathbf{A}}^{\circ}_{ik}\mathbf{b}^{\circ}_{ik} + \sigma_n^2\mathbf{i}, & i = k, \end{cases} \tag{28}$$

where $\bar{\mathbf{A}}^{\circ}_{ik}$ is defined as the collection of steering vectors $\bar{\mathbf{a}}_{ik}(\alpha_g)$ over all possible grids α_g, $g = 1, \ldots, G_\alpha$, with $G_\alpha \gg Q$, and $\mathbf{b}^{\circ}_{ik}$ is the sparse vector whose non-zero entry positions correspond to the DOAs of the estimates of α_q, $q = 1, \ldots, Q$. For different subarray pairs, the non-zero entries generally have distinct values but share the same positions in the searching. That is, $\mathbf{b}^{\circ}_{ik}$ exhibits a group sparsity across all subarray pairs. Thus, the estimation of α_q, $q = 1, \ldots, Q$, can be solved in the group sparse reconstruction framework [48], and all DOFs in self- and cross-lag can be fully used. A number of effective algorithms within the convex optimization [49,50] and Bayesian sparse learning [51] frameworks are available to solve the complex-valued group sparse reconstruction problem. In this paper, the complex multitask Bayesian compressive sensing (CMT-BCS) algorithm proposed in [52] and summarized below is used due to its superior performance and robustness to dictionary coherence.

In order to exploit both self- and cross-lags, we reformulate the vectors $\mathbf{z}_{ik}$ as:

$$\mathbf{z}_{ik} = \mathbf{\Phi}^{\circ}_{ik}\bar{\mathbf{b}}^{\circ}_{ik} + \boldsymbol{\epsilon}_{ik}, \quad 1 \le i, k \le 3, \tag{29}$$

where each vector $\mathbf{z}_{ik}$ employs its respective dictionary matrix,

$$\mathbf{\Phi}^{\circ}_{ik} = \begin{cases} \left[\bar{\mathbf{A}}^{\circ}_{ik}, \mathbf{i}\right], & i = k, \\ \left[\bar{\mathbf{A}}^{\circ}_{ik}, \mathbf{0}_{N_t^i N_t^k \times 1}\right], & i \neq k. \end{cases} \tag{30}$$

Note that the dimension of the unknown sparse vector is expanded to $\bar{\mathbf{b}}^{\circ}_{ik}$ by an additional element of the noise power σ_n^2. In this case, the first G_α elements of the obtained estimates of $\bar{\mathbf{b}}^{\circ}_{ik}$ are used to determine the α_q, whereas the last element is discarded. Furthermore, an error vector $\boldsymbol{\epsilon}_{ik}$ is included in (29) to account for the discrepancies between the statistical expectation and the sample average in computing the covariance matrices. The discrepancies are modelled as i.i.d. complex Gaussian as a result of a sufficiently large number of samples employed in the averaging.

Assume that the entries in $\bar{\mathbf{b}}^{\circ}_{ik}$ are drawn from the product of the following zero-mean Gaussian distributions:

$$\bar{\mathbf{b}}^{\circ g}_{ik} \sim \mathcal{N}(\bar{\mathbf{b}}^{\circ g}_{ik} | \mathbf{0}, \gamma_g \mathbf{I}_2), \quad g \in [1, \ldots, G_\alpha], \tag{31}$$

where $\bar{\mathbf{b}}^{\circ g}_{ik} = [\tilde{b}^{\circ g_R}_{ik} \ \tilde{b}^{\circ g_I}_{ik}]^T$ is a 2×1 vector consisting of the real part coefficient $\tilde{b}^{\circ g_R}_{ik}$ and the imagery part coefficient $\tilde{b}^{\circ g_I}_{ik}$, corresponding to the gth grid. It is easy to confirm that the $\bar{\mathbf{b}}^{\circ g}_{ik}$ trends to be zero when γ_g is set to zero [53–55]. To encourage the sparsity of $\bar{\mathbf{b}}^{\circ}_{ik}$, a Gamma prior is placed on $\gamma_g^{-1} \sim \text{Gamma}(\gamma_g^{-1} | a, b)$, where $\text{Gamma}(x^{-1}|a,b) = \Gamma(a)^{-1} b^a x^{-(a-1)} e^{-\frac{b}{x}}$, with $\Gamma(\cdot)$ denoting the Gamma function, and a and b are hyper-parameters. Vector $\boldsymbol{\gamma} = [\gamma_1, \ldots, \gamma_G]^T$ contains the variances of entries $\bar{\mathbf{b}}^{\circ g}_{ik}$ for all $g = 1, \ldots, G_\alpha$ and is shared by all groups to enforce the group sparsity. Likewise, a Gaussian prior $\mathcal{N}(\mathbf{0}, \xi_0 \mathbf{I}_2)$ is also placed on $\boldsymbol{\epsilon}_{ik}$ and the Gamma prior is placed on ξ_0^{-1} with hyper-parameters c and d.

Define two $G_\alpha \times 1$ vectors $\bar{\mathbf{b}}^{\circ R}_{ik} = [b^{\circ 1R}_{ik}, \ldots, b^{\circ GR}_{ik}]^T$ and $\bar{\mathbf{b}}^{\circ I}_{ik} = [b^{\circ 1I}_{ik}, \ldots, b^{\circ GI}_{ik}]^T$, the joint posterior density function of $\bar{\mathbf{b}}^{\circ RI}_{ik} = [(\bar{\mathbf{b}}^{\circ R}_{ik})^T, (\bar{\mathbf{b}}^{\circ I}_{ik})^T]^T$ can be evaluated as

$$\Pr(\bar{\mathbf{b}}^{\circ RI}_{ik} | \bar{\mathbf{z}}_{ik}, \mathbf{\Phi}^{\circ}_{ik}, \boldsymbol{\gamma}, \xi_0) = \mathcal{N}(\bar{\mathbf{b}}^{\circ RI}_{ik} | \boldsymbol{\mu}_{ik}, \mathbf{\Sigma}_{ik}), \tag{32}$$

where

$$\bar{\mathbf{z}}^{RI}_{ik} = \left[\text{Re}(\mathbf{z}_{ik})^T, \text{Im}(\mathbf{z}_{ik})^T\right]^T \tag{33}$$

$$\boldsymbol{\mu}_{ik} = \xi_0^{-1} \mathbf{\Sigma}_{ik} \mathbf{\Psi}_{ik}^T \bar{\mathbf{z}}^{RI}_{ik}, \tag{34}$$

$$\mathbf{\Sigma}_{ik} = \left[\xi_0^{-1} \mathbf{\Psi}_{ik}^T \mathbf{\Psi}_{ik} + \mathbf{F}^{-1}\right]^{-1}, \tag{35}$$

$$\mathbf{\Psi} = \begin{bmatrix} \text{Re}(\mathbf{\Phi}^{\circ}_{ik}) & -\text{Im}(\mathbf{\Phi}^{\circ}_{ik}) \\ \text{Im}(\mathbf{\Phi}^{\circ}_{ik}) & \text{Re}(\mathbf{\Phi}^{\circ}_{ik}) \end{bmatrix}, \tag{36}$$

$$\mathbf{F} = \text{diag}(\gamma_1, \ldots, \gamma_G, \gamma_1, \ldots, \gamma_{G_\alpha}). \tag{37}$$

It is clear that the mean and variance of each scattering coefficients in $\bar{\mathbf{b}}^{\circ RI}_{ik}$ can be derived using (34) and (35) when γ and ξ_0 are given. On the other hand, the values of γ and ξ_0 are determined by maximizing the logarithm of the marginal likelihood, which can be implemented via the expectation maximization (EM) algorithm to yield

$$\gamma_g^{(\text{new})} = \frac{1}{9} \sum_{i,k=1}^{3} \left(\mu^2_{ik,g} + \mu^2_{ik,g+G_\alpha} + \Sigma_{ik,gg} + \Sigma_{ik,(g+G_\alpha)(g+G_\alpha)}\right), \tag{38}$$

$$\xi_0^{(\text{new})} = \frac{1}{18 G_\alpha} \sum_{i,k=1}^{3} \left(\text{Tr}[\mathbf{\Sigma}_{ik} \mathbf{\Psi}_{ik}^T \mathbf{\Psi}_{ik}] + ||\tilde{\mathbf{z}}^{RI}_{ik} - \mathbf{\Psi}_{ik} \boldsymbol{\mu}_{ik}||_2^2\right), \tag{39}$$

where $\mu_{ik,g}$ and $\mu_{ik,g+G_\alpha}$ are the gth and $(g+G_\alpha)$th elements in vector $\boldsymbol{\mu}_{ik}$, and $\Sigma_{ik,gg}$ and $\Sigma_{ik,(g+G_\alpha)(g+G_\alpha)}$ are the (g, g) and $(g+G_\alpha, g+G_\alpha)$ entries in matrix $\mathbf{\Sigma}_{ik}$. Because $\boldsymbol{\gamma}$ and ξ_0 depend on $\boldsymbol{\mu}_{ik}$ and $\mathbf{\Sigma}_{ik}$, the CMT-BCS algorithm is iterative and iterates between (34), (35) and (38), (39) until a convergence criterion is reached. The estimates $\hat{\alpha}_q$, $q = 1, \ldots, Q$, can be obtained corresponding to the Q largest values in $\sum_{i,k=1}^{3} (b^{\circ gR}_{ik} + b^{\circ gI}_{ik})$, $g = 1, \ldots, G$. Then, the $Q \times 1$ vector in (25), i.e., $\mathbf{b}_{ik}$, $i \neq k$, can be estimated by least squares (LS) fitting, expressed as

$$\hat{\mathbf{b}}_{ik} = \left(\hat{\bar{\mathbf{A}}}_{ik}^H \hat{\bar{\mathbf{A}}}_{ik}\right)^{-1} \hat{\bar{\mathbf{A}}}_{ik}^H \mathbf{z}_{ik}, \quad i \neq k, \tag{40}$$

where

$$\bar{\mathbf{A}}_{ik} = [\bar{\mathbf{a}}_{ik}(\hat{\alpha}_1), \ldots, \bar{\mathbf{a}}_{ik}(\hat{\alpha}_Q)]. \tag{41}$$

As such, β_q, $q = 1, \ldots, Q$ are estimated by

$$\hat{\beta}_q = \cos^{-1}\left(-\text{phase}(\hat{b}_q)/\pi\right), \tag{42}$$

where $\hat{b}_q$ is the qth element of vector $\hat{\mathbf{b}}_{ik}$, and $\hat{\beta}_q$ is thus automatically paired with the corresponding $\hat{\alpha}_q$. In the end, the elevation and azimuth angles, $\hat{\theta}_q$ and $\hat{\phi}_q$, can be obtained with (21) and (22).

Note that the proposed difference coarray based approach enables to resolve more sources than the number of sensors. While it also works for the case of $Q < N_t$, the corresponding estimation accuracy is interior to the counterpart described in previous section because of the errors in the estimated covariance matrix, particularly when the number of data snapshots is not sufficiently high [56].

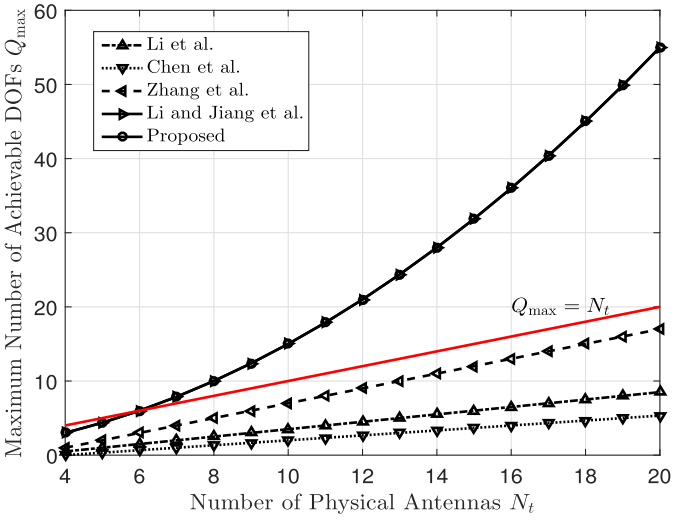

Fig. 3. $Q_{\max}$ versus N_t.

5. Number of DOFs and computational complexity

5.1. Analysis of DOFs

In the proposed approach, the resulting coarray is equivalent to the conventional coprime array in the 1-D case. That is, the achievable number of estimated signals $Q_{\text{av}} = MN$. For a given number of physical antennas $N_t = 2M + N - 1$, Q_{av} can be optimized by:

$$\begin{aligned} &\text{Maximize} \quad Q_{\text{av}} = MN \\ &\text{subject to} \quad N_t = 2M + N - 1, \\ &\qquad\qquad M < N, \quad M, N \in \mathbb{N}^+. \end{aligned} \tag{43}$$

It is evident that the valid optimal coprime pair is the one that has $2M$ and N as close as possible. This is satisfied by choosing $M = \lfloor (N_t - 1)/4 \rfloor$. In this case, the maximum number of estimated signals Q_{av} is given by

$$Q_{\max} = \left\lfloor \frac{N_t (N_t + 2)}{8} \right\rfloor. \tag{44}$$

In Fig. 3, we compare the value of $Q_{\max}$ in the proposed approach with those obtained using the methods described in [10,12,13,46], which are referred to as Li et al., Chen et al., Zhang et al., and Li and Jiang et al., respectively, in the plots. While $Q_{\max}$ increases with N_t in all methods, it is clear that the coprime structure-based approaches (the proposed method and that proposed by Li and Jiang et al.) significantly outperform other approaches. In particular, when $N_t > 6$, the coprime structure-based approaches resolve more sources than the number of array sensors, whereas for other methods, the number of resolvable sources is less than the number of sensors.

5.2. Analysis of computational complexity

Here, we compare their computational complexity using the same number of array elements N_t. When the number of sources Q is smaller than the number of sensors, i.e., $Q < N_t$, the complexity of the proposed approach mainly includes four parts: computation of the covariance matrix, eigenvalue decomposition, estimation of azimuth angles using RARE, and estimation of elevation angles using 1-D MUSIC-like search. Thus, the resulting total computational load is $\mathcal{O}(N_t^2 T + N_t^3 + G_\alpha N_t + G_\beta N_t^2) \approx \mathcal{O}(N_t^2 T)$, which is far less than that of the 2-D MUSIC counterpart, given as $\mathcal{O}(N_t^2 T + N_t^3 + G_\alpha G_\beta N_t^2) \approx \mathcal{O}(G_\alpha G_\beta N_t^2)$, under typical circumstances such that $G_\alpha G_\beta \gg T \gg N_t > Q$, where T, G_α and G_β are the number of snapshots, the number of search grids in azimuth and elevation angles, respectively. As a comparison, the methods proposed in [10,12,13] require a similar $\mathcal{O}(N_t^2 T)$ complexity when $T \gg N_t > Q$. However, the available number of DOFs in these papers are lower than that of the proposed coprime structure-based approaches. While both [46] and the proposed approach can resolve the case of $Q > N_t$ through the coarray with a complexity of $\mathcal{O}(G_\alpha^2 N_t^2)$ in the context of sparse reconstruction, the proposed approach outperforms the method proposed by Li and Jiang et al. in [46] due to the benefits of the array design with a larger aperture as well as the group sparsity-based algorithm.

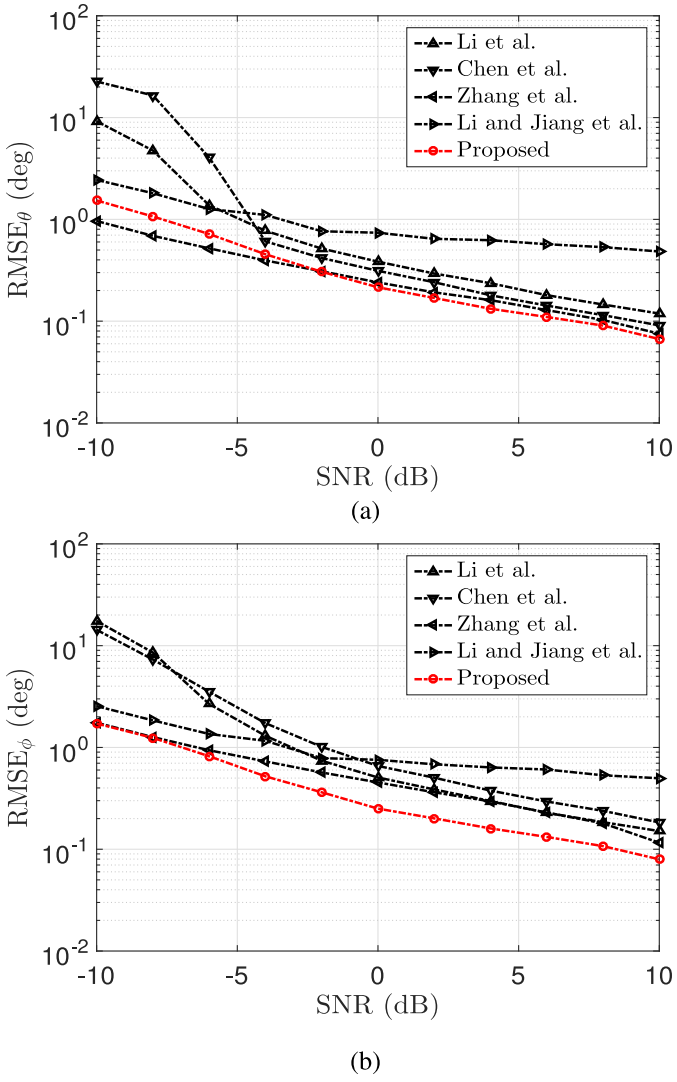

Fig. 4. RMSE versus SNR ($Q = 2$). (a) RMSE_θ; (b) RMSE_ϕ.

6. Simulation results

For illustration, we consider 2-D DOA estimation based on the proposed approach. We set $M = 3$ and $N = 8$, leading to an array configuration of $N_t = 2M + N - 1 = 13$ antennas. In addition, $L = 20$ is assumed. Q far-field sources with identical power are assumed to be on elevation-azimuth plane (θ_q, ϕ_q), where $\theta_q \in [0^\circ, 90^\circ]$ and $\phi_q \in [-90^\circ, 90^\circ]$, for $q = 1, \ldots, Q$. The grid interval in the angular space is set to 0.2°, and the hyper-parameters in group Bayesian sparse learning is set to $a = b = c = d = 0$.

In Figs. 4 and 5, we first examine the estimation accuracy and compare it with Li et al. [10], Chen et al. [12], Zhang et al. [13],

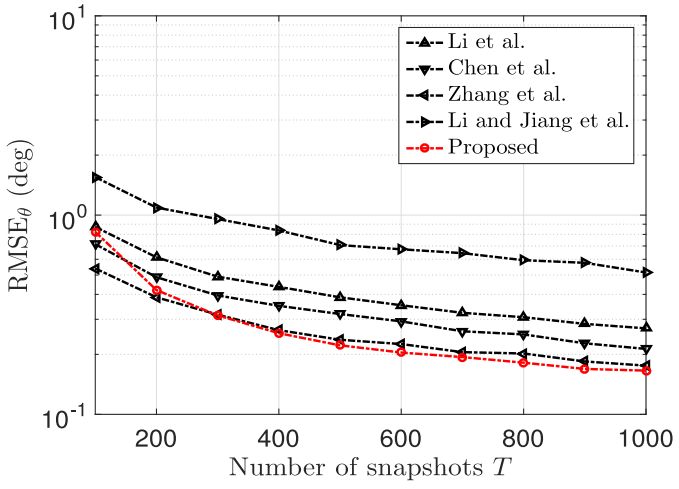

(a)

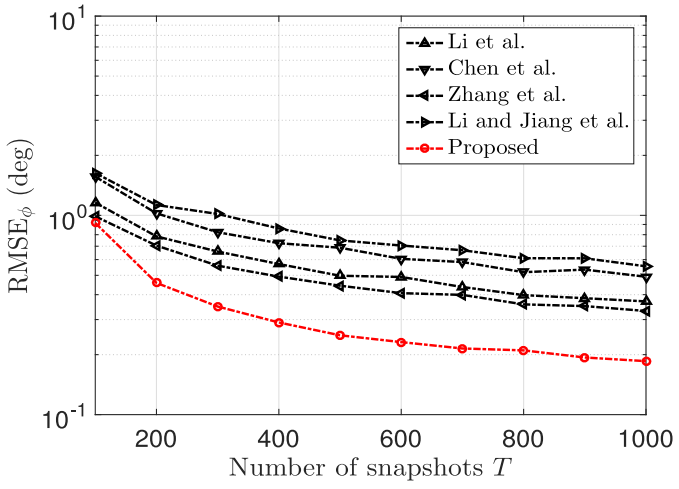

(b)

Fig. 5. RMSE versus T ($Q = 2$). (a) RMSE$_\theta$; (b) RMSE$_\phi$.

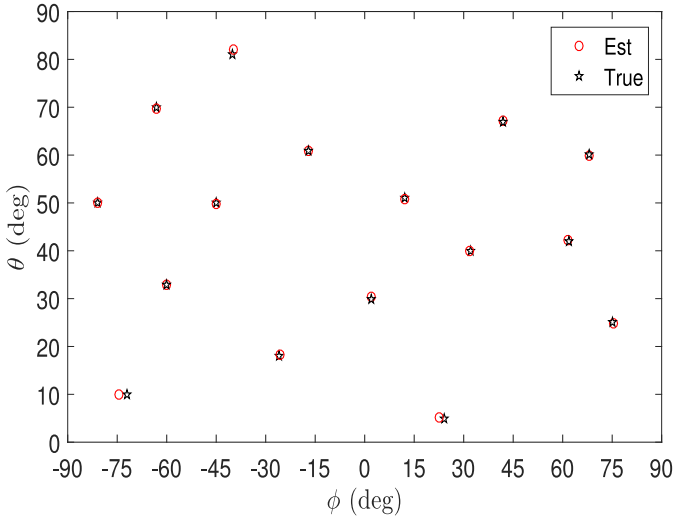

(a)

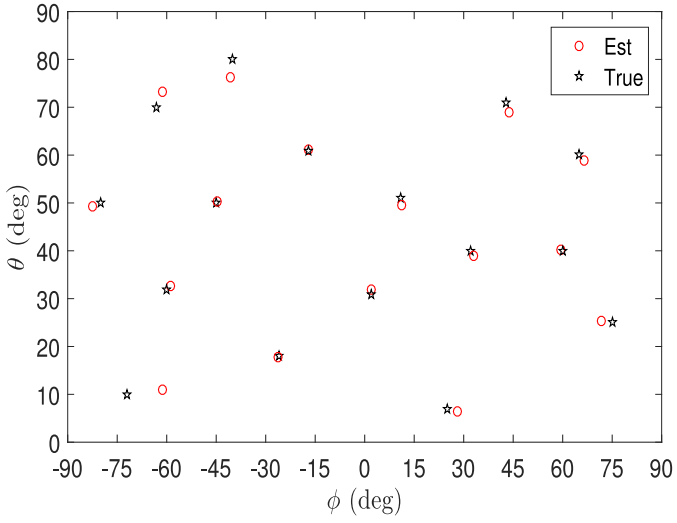

(b)

Fig. 6. 2-D DOA estimation results ($Q = 16$). (a) The proposed approach; (b) The method by Li and Jiang et al..

and Li and Jiang et al. [46]. The average root mean square error (RMSE) of the estimated azimuth and elevation angles, respectively expressed as

$$\text{RMSE}_\theta = \sqrt{\frac{1}{IQ}\sum_{i=1}^{I}\sum_{q=1}^{Q}(\hat{\theta}_q(i)-\theta_q)^2},$$
$$\text{RMSE}_\phi = \sqrt{\frac{1}{IQ}\sum_{i=1}^{I}\sum_{q=1}^{Q}(\hat{\phi}_q(i)-\phi_q)^2}, \tag{45}$$

are used as the performance metric, where $\hat{\theta}_q(i)$ and $\hat{\phi}_q(i)$ are the estimates of θ_q and ϕ_q for the ith Monte Carlo trial, $i = 1, \ldots, I$.

In the first set of simulation, we consider the case $Q < N_t$. To enable a feasible comparison, $Q = 2 < N_t = 13$ sources impinging from $(40^\circ, 32^\circ)$ and $(19^\circ, -26^\circ)$ are considered so that all methods have sufficient DOFs for correct identification. We use $I = 500$ independent trials in the simulations. Fig. 4 compares the RMSE performance as a function of input signal-to-noise ratio (SNR), where $T = 500$ snapshots are used. Fig. 5 compares the performance with respect to the number of snapshots, with input SNR set to 0 dB. In both figures, it is evident that the proposed approach outperforms the other methods. The estimation accuracy of the coarray based method (i.e., by Li and Jiang et al.) is inferior to other subspace-based approaches due to discrepancies between the statistical expectation and the sample average in the computed covariance matrices $\mathbf{R}_{i,k}$ when extracting the virtual array. Also, the estimates of both θ and ϕ are improved with the increased SNR and the number of snapshots.

In the second set of simulation, we consider a scenario with $Q = 16$ sources as an example for the $Q > N_t$ case, and the results are depicted in Fig. 6. In this case, the number of sources is higher than N_t as well as the available DOFs offered by the methods in [10,12,13]. Therefore, the performance of these methods are not depicted. Only the proposed difference coarray based approach successfully resolve all sources, as shown in Fig. 6. In this simulation, the input SNR remains 0 dB, whereas the number of snapshots is increased to 5000 to further demonstrate the capability of the proposed method in dealing with a high number of sources. Compared to the method by Li and Jiang et al., the proposed array configuration increases the aperture in the elevation domain to achieve an improved elevation angle resolution. Moreover, the group spar-

sity makes fully utilization of data across all vectorized covariance matrices. The proposed technique thus outperforms that of Li and Jiang et al., as presented in Fig. 6.

7. Conclusions

In this paper, a novel coprime array configuration with parallel subarrays was proposed for 2-D DOA estimation. Two effective schemes were introduced, each is applicable to a different scenario involving the number of sources in relation to the number of sensors. In both cases, the 2-D DOA estimation was decomposed into two separate 1-D problems where the estimates of the elevation and azimuth angles were paired automatically avoiding any problem with associations. The proposed method resolves 2-D signals DOAs and the number of detectable sources is the same as conventional coprime arrays which only resolve 1-D signal DOAs. The effectiveness of the proposed method was demonstrated by simulations that showed the capability of resolving a large number of sources with high angle estimation accuracy.

Declaration of Competing Interest

The authors declare that they have no known competing financial interests or personal relationships that could have appeared to influence the work reported in this paper.

References

[1] H.L. Van Trees, Detection, Estimation, and Modulation Theory, Optimum Array Processing, John Wiley & Sons, 2004.
[2] R. Schmidt, Multiple emitter location and signal parameter estimation, IEEE Trans. Antennas Propag. 34 (3) (1986) 276–280.
[3] R. Roy, T. Kailath, ESPRIT – estimation of signal parameters via rotation invariance techniques, IEEE Trans. Acoust. Speech Signal Process. 37 (7) (1989) 984–995.
[4] S. Marcos, A. Marsal, M. Benidir, The propagator method for source bearing estimation, Signal Process. 42 (2) (1995) 121–138.
[5] H. Huang, J. Yang, H. Huang, Y. Song, G. Gui, Deep learning for super-resolution channel estimation and DOA estimation based massive MIMO system, IEEE Trans. Veh. Technol. 67 (9) (2018) 8549–8560.
[6] J.W. Odendaal, E. Barnard, C.W.I. Pistorius, Two-dimensional superresolution radar imaging using the MUSIC algorithm, IEEE Trans. Antennas Propag. 42 (10) (1994) 1386–1391.
[7] J. Li, R.T. Compton, Two-dimensional angle and polarization estimation using the ESPRIT algorithm, IEEE Trans. Antennas Propag. 40 (5) (1992) 550–555.
[8] P. Li, B. Yu, J. Sun, A new method for two-dimensional array signal processing in unknown noise enviroments, Signal Process. 47 (3) (1995) 319–327.
[9] Y. Wu, G. Liao, H.C. So, A fast algorithm for 2-D direction-of-arrival estimation, Signal Process. 83 (8) (2003) 1827–1831.
[10] J. Li, X. Zhang, H. Chen, Improved two-dimensional DOA estimation algorithm for two-parallel uniform linear arrays using propagator method, Signal Process. 92 (12) (2012) 3032–3038.
[11] N. Tayem, H.M. Kwon, Azimuth and elevation angle estimation with no failure and no eigen decomposition, Signal Process. 86 (1) (2006) 8–16.
[12] H. Chen, C. Hou, Q. Wang, L. Huang, W. Yan, L. Pu, Improved azimuth/elevation angle estimation algorithm for three-parallel uniform linear arrays, IEEE Antennas Wirel. Propag. Lett. 14 (1) (2014) 329–332.
[13] Y. Zhang, X. Xu, Y.A. Sheikh, Z. Ye, A rank-reduction based 2-D DOA estimation algorithm for three parallel uniform linear arrays, Signal Process. 120 (1) (2016) 305–310.
[14] M. Pesavento, A.B. Gershman, K.M. Wong, Direction finding in partly calibrated sensor arrays composed of multiple subarrays, IEEE Trans. Signal Process. 50 (9) (2002) 2103–2115.
[15] S. Pillai, Array Signal Processing, Springer, 1989.
[16] R.T. Hoctor, S.A. Kassam, The unifying role of the coarray in aperture synthesis for coherent and incoherent imaging, Proc. IEEE 78 (4) (1990) 735–752.
[17] P.P. Vaidyanathan, P. Pal, Sparse sensing with co-prime samplers and arrays, IEEE Trans. Signal Process. 59 (2) (2011) 573–586.
[18] P. Pal, P.P. Vaidyanathan, Coprime sampling and the MUSIC algorithm, in: Proc. IEEE Digital Signal Process. Workshop and IEEE Signal Process. Educ. Workshop (DSP/SPE), Sedona, AZ, 2011, pp. 289–294.
[19] P. Pal, P.P. Vaidyanathan, Nested arrays: a novel approach to array processing with enhanced degrees of freedom, IEEE Trans. Signal Process. 58 (8) (2010) 4167–4181.
[20] Q. Wu, Q. Liang, Coprime sampling for nonstationary signal in radar signal processing, EURASIP J. Wirel. Commun. Netw. (2013), doi:10.1186/1687-1499-2013-58.
[21] J. Chen, Q. Liang, B. Zhang, X. Wu, Spectrum efficiency of nested sparse sampling and coprime sampling, EURASIP J. Wirel. Commun. Netw. (2013), doi:10.1186/1687-1499-2013-47.
[22] Z. Tan, A. Nehorai, Sparse direction-of-arrival estimation using co-prime arrays with off-grid targets, IEEE Signal Process. Lett. 21 (1) (2014) 26–29.
[23] K. Adhikari, J.R. Buck, K.E. Wage, Extending coprime sensor arrays to achieve the peak side lobe height of a full uniform linear array, EURASIP J. Wirel. Commun. Netw. (2014), doi:10.1186/1687-6180-2014-148.
[24] Z. Tan, Y.C. Eldar, A. Nehorai, Direction of arrival estimation using co-prime arrays: a super resolution viewpoint, IEEE Trans. Signal Process. 62 (21) (2014) 5565–5576.
[25] S. Qin, Y.D. Zhang, Q. Wu, M.G. Amin, Structure-aware Bayesian compressive sensing for near-field source localization based on sensor-angle distributions, Int. J. Antennas Propag. 2015 (2015). Article ID 783467
[26] E. Boudaher, Y. Jia, F. Ahmad, M.G. Amin, Multi-frequency co-prime arrays for high-resolution direction-of-arrival estimation, IEEE Trans. Signal Process. 63 (14) (2015) 3797–3808.
[27] C.-L. Liu, P.P. Vaidyanathan, Remarks on the spatial smoothing step in coarray MUSIC, IEEE Signal Process. Lett. 22 (9) (2015) 1438–1442.
[28] C.-L. Liu, P.P. Vaidyanathan, Super nested arrays: linear sparse arrays with reduced mutual coupling - Part I: fundamentals, IEEE Trans. Signal Process. 64 (15) (2016) 3997–4012.
[29] C.-L. Liu, P.P. Vaidyanathan, Super nested arrays: linear sparse arrays with reduced mutual coupling - Part II: high-order extensions, IEEE Trans. Signal Process. 64 (16) (2016) 4203–4217.
[30] S. Qin, Y.D. Zhang, M.G. Amin, B. Himed, DOA estimation exploiting a uniform linear array with multiple co-prime frequencies, Signal Process. 130 (2017) 37–46.
[31] S. Qin, Y.D. Zhang, M.G. Amin, A.M. Zoubir, Generalized coprime sampling of Toeplitz matrices for spectrum estimation, IEEE Trans. Signal Process. 65 (1) (2017) 81–94.
[32] S. Qin, Y.D. Zhang, M.G. Amin, F. Gini, Frequency diverse coprime arrays with coprime frequency offsets for multi-target localization, IEEE J. Sel. Top. Signal Process. 11 (2) (2017) 321–335.
[33] S. Qin, Y.D. Zhang, M.G. Amin, DOA estimation of mixed coherent and uncorrelated targets exploiting coprime MIMO radar, Digit. Signal Process. 61 (2017) 26–34.
[34] C.-L. Liu, P.P. Vaidyanathan, Correlation subspaces: generalizations and connection to difference coarrays, IEEE Trans. Signal Process. 65 (19) (2017) 5006–5020.
[35] R. Bautista, J.R. Buck, Statistical characterization of coprime sensor arrays: array gain vs. spatially correlated noise, J. Acoust. Soc. Am. 141 (5) (2017) 3843.
[36] H. Huang, B. Liao, X. Wang, X. Guo, J. Huang, A new nested array configuration with increased degrees of freedom, IEEE Access 6 (2018) 1490–1497.
[37] H. Huang, B. Liao, Q. Shen, DOA estimation of quasi-stationary signals with a nested array in unknown noise field, in: Proc. IEEE SAM, Sheffield, UK, 2018, pp. 41–45.
[38] I.M. Rooney, Y. Liu, J.R. Buck, Spatial power spectral density estimation using a multitapered coprime sensor array minimum processor, J. Acoust. Soc. Am. 143 (6) (2018) 3959–3971.
[39] Y. Liu, J.R. Buck, Gaussian source detection and spatial spectral estimation using a coprime sensor array with the min processor, IEEE Trans. Signal Process. 66 (1) (2018) 186–199.
[40] R. Bautista, J.R. Buck, Processor dependent bias of spatial spectral estimates from coprime sensor arrays, J. Acoust. Soc. Am. 143 (6) (2018) 3972–3978.
[41] M. Yang, L. Sun, X. Yuan, B. Chen, A new nested MIMO array with increased degrees of freedom and hole-free difference coarray, IEEE Signal Process. Lett. 25 (1) (2018) 40–44.
[42] M. Yang, A.M. Haimovich, X. Yuan, L. Sun, B. Chen, A unified array geometry composed of multiple identical subarrays with hole-free difference coarrays for underdetermined DOA estimation, IEEE Access 6 (2018) 14238–14254.
[43] R. Bautista, J.R. Buck, Detection gaussian signals using coprime sensor arrays in spatially correlated gaussian noise, IEEE Trans. Signal Process. 67 (5) (2019) 1296–1306.
[44] S. Qin, Y.D. Zhang, M.G. Amin, Generalized coprime array configurations for direction-of-arrival estimation, IEEE Trans. Signal Process. 63 (6) (2015) 1377–1390.
[45] S. Qin, Y.D. Zhang, M.G. Amin, Two-dimensional DOA estimation using parallel coprime subarrays, in: Proc. IEEE Sens. Array Multichannel Signal Process. Workshop (SAM), Rio de Janeiro, Brazil, 2016.
[46] J. Li, D. Jiang, X. Zhang, Sparse representation based two-dimensional direction of arrival estimation using co-prime array, Multidimens. Syst. Signal Process. (2016), doi:10.1007/s11045-016-0453-9.
[47] F. Sun, P. Lan, B. Gao, G. Zhang, An efficient dictionary learning-based 2-D DOA estimation without pair matching for co-prime parallel arrays, IEEE Access 6 (2018) 8510–8518.
[48] J. Huang, T. Zhang, The benefit of group sparsity, Ann. Stat. 38 (4) (2010) 1978–2004.
[49] D.L. Donoho, Compressed sensing, IEEE Trans. Inf. Theory 52 (4) (2006) 1289–1306.
[50] M. Yuan, Y. Lin, Model selection and estimation in regression with grouped variables, J. R. Stat. Soc. Ser. B 68 (1) (2006) 49–67.
[51] S. Ji, D. Dunson, L. Carin, Multitask compressive sensing, IEEE Trans. Signal Process. 57 (1) (2009) 92–106.
[52] Q. Wu, Y.D. Zhang, M.G. Amin, Complex multitask Bayesian compressive sens-

ing, in: Proc. IEEE Int. Conf. Acoust. Speech Signal Process. (ICASSP), Florence, Italy, May, 2014, pp. 3375–3379.
[53] M.E. Tipping, Sparse Bayesian learning and the relevance vector machine, J. Mach. Learn. Res. 1 (9) (2001) 211–244.
[54] S. Ji, Y. Xue, L. Carin, Bayesian compressive sensing, IEEE Trans. Signal Process. 56 (6) (2008) 2346–2356.
[55] D.J.C. MacKay, Bayesian interpolation, Neural Comput. 4 (3) (1992) 415–447.
[56] C.-L. Liu, P.P. Vaidyanathan, Cramér-Rao bounds for coprimeand other sparse arrays, which find more sources than sensors, Digit. Signal Process. 61 (2017) 43–61.